Fundamentals of Spatial Vision

James A. Ferwerda
Program of Computer Graphics
Cornell University

1 Visual anatomy and physiology

1.1 The eye

The adult human eye is aproximately 25mm in diameter and weighs about 7g. The anterior section of the eye contains the eye's optical system whose major structures are the *cornea*, *lens*, and *iris*. The cornea provides about two-thirds of the eye's refractive power, but the lens provides fine focus for targets at distances from 20 feet down to about 4 inches (Pugh88). The ciliary muscles attached to edge of the lens effect focusing by changing the len's shape. The space between the lens and the cornea is filled with a fluid known as the *aqueous humor*. The iris sits just in front of the lens and has a central aperture known as the pupil that admits light to the eye. The central cavity of the eyeball is filled with a fluid called the *vitreous humor*.

The posterior section of the eyeball contains its neural structures. This section is composed of three layers. The *sclera* is a tough covering that protects the interior from damage and helps to maintain the eye's shape. The *choroid* is a middle layer that provides the blood supply to the eye's internal structures. The *retina* is the innermost layer that contains light sensitive photoreceptors and associated neural tissue.

About 4% of the light incident on the eye is absorbed or reflected by the cornea. Absorption or scattering by the internal structures of the eye means that only about 50% of the light coming to the eye actually reaches the photosensitive retinal surface.

1.2 The retina

The retina is composed of two major classes of receptor cells known as *rods* and *cones* due to the shapes of their photosensitive outer segments. There are somewhere between 100-120 million rods and 7-8 million cones in each retina. The rods are extremely sensitive to light and provide achromatic vision at low (*scotopic*) levels of illumination. The cones are less sensitive than the rods, but provide color vision at high (*photopic*) levels of illumination. The photosensitive segments of the rods and cones are located closest to the choroid layer. This means that light striking the retina must first pass through several layers of neural tissue to reach the photoreceptors. Only in a small 1.5mm diameter area near the optic axis called the *fovea* are the cell bodies and neural fibers drawn aside so the photoreceptive surfaces are directly exposed to light.

The rod and cone systems are sensitive to light with wavelengths from about 400nm to 700nm. The rods have their peak sensitivity at approximately 498nm. There are three classes of cones with bandpass spectral response characteristics. The short wavelength or "blue" cones have have their peak response at 420nm, the medium wavelength or "green" cones peak at 534nm, and the long wavelength or "red" cones peak at 564nm. There is significant overlap between the response ranges of the different classes of cones. This means that spectrally broadband stimuli will simultaneously activate multiple classes of cones. Sensitivity of the composite cone system peaks at 555nm.

The rods and cones are not distributed equally over the surface of the retina. The fovea has the densest packing of medium and long wavelength cones, but is nearly devoid of rods and short wavelength cones. Cone density falls off in a nearly exponential manner with increasing eccentricity from the fovea and asymptotes to a constant low level at about 20 degrees from the fovea. In contrast rod density increase from near zero in the fovea to a maximum at 20 degrees away from the fovea. Rod density decreases with further increases in eccentricity and both rods and cones reach their minimum levels at 75 to 80 degrees away from the fovea.

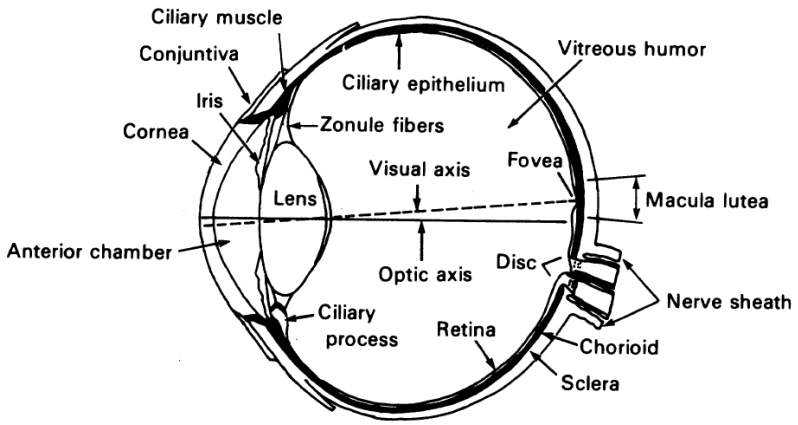

Figure 1: Structures of the human eye. From (Atkinson86) after (Walls42).

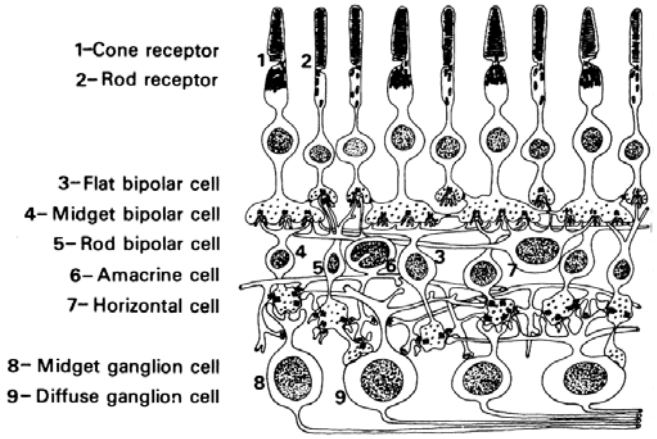

Figure 2: Cross section of the primate retina. From (Atkinson86) after (Dowling66).

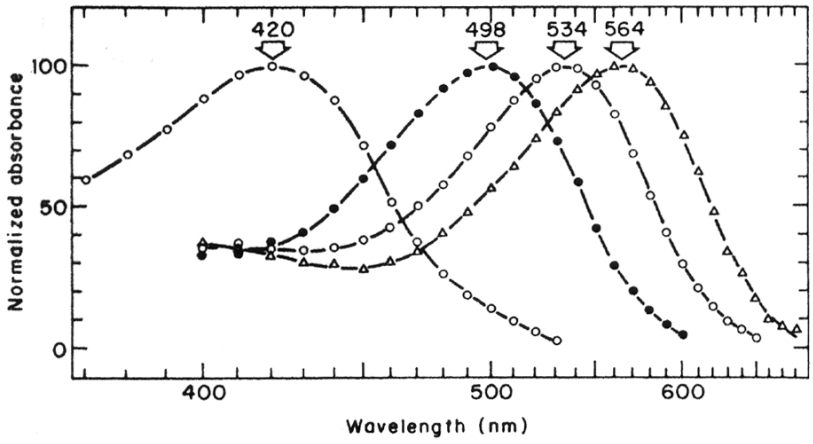

Figure 3: Spectral response properties of the rods and cones. From (Gordon89) after (Bowmaker80).

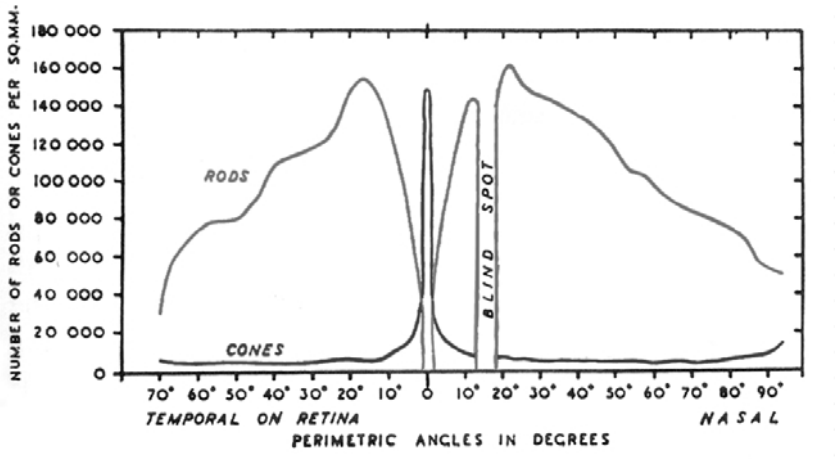

Figure 4: Distribution of rods and cones in the retina. From (Pirenne67).

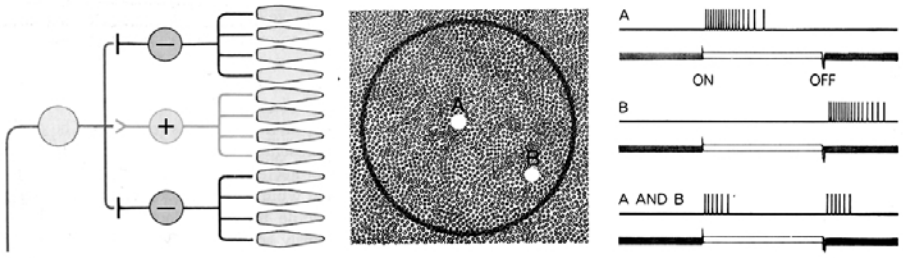

Figure 5: Functional architecture and response properties of an on-center ganglion cell. From (Michael69) and (Kennedy63).

1.2.1 The plexiform layers

The rods and cones synapse on a network of neurons in the outer and inner *plexiform layers* of the retina. The cells in the plexiform layers connect groups of rods and cones to *ganglion cells* whose axons make up the fibers of the optic nerve. The spatially localized group of photoreceptors that serve a particular ganglion cell make up what is called the cell's *receptive field*.

The plexiform layers provide both direct and lateral interconnections from receptor to ganglion cell. Receptors synapse on *bipolar cells* which in turn synapse on ganglion cells. *Horizontal cells* in the outer plexiform layer provide lateral interconnections between receptors *Amacrine cells* in the inner plexiform layer provide lateral interconnections between bipolar cells and ganglion cells.

The plexiform layers appear to be made up of a number of functional subsystems that serve scotopic and photopic vision as well as other visual functions. Three classes of bipolar cells (midget, flat, and rod) and two classes of ganglion cells (midget and diffuse) have been identified through histological and electrophysiological studies. The most direct mapping from receptor to optic nerve fiber occurs in the fovea where single cones synapse on midget bipolars which in turn synapse on midget ganglion cells. Groups of cones may also synapse on flat bipolar cells which in turn synapse on diffuse ganglion cells. Rods synapse on rod bipolar cells which in turn synapse on diffuse ganglion cells. Thus there is physiological evidence in support of a structural separation between the rod and cone systems but there is also evidence for some degree of interconnection between the systems. What role this organization plays visual perception is still a topic of research.

1.2.2 Retinal ganglion cells

The receptive fields of ganglion cells are the basic units of higher visual function. Electrophysiological studies of the cat have shown that many ganglion cell receptive fields have an antagonistic center surround

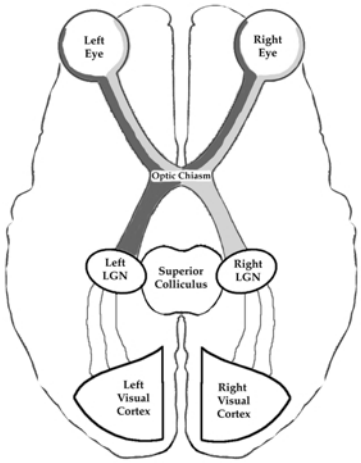

Figure 6: Visual pathways: retina to cortex. After (Sekuler94).

organization (Kuffler53). The activation produced by stimulation in the center of a cells receptive field tends to be suppressed by stimulation in the annular surround. Uniform stimulation over the whole receptive field generally produces only a weak response from the ganglion cell.

Two functional classes of ganglion cell receptive fields have been identified. *On-center cells* increase their firing rate in response to increments of light in the centers of their receptive fields, and *off-center* cells increase firing rate in response to light decrements. The antagonistic organization of receptive fields shows that very early on in the visual system information for the absolute intensity of visual stimulation is lost and only contrast is signaled to later stages of visual processing. This view has significant implications for theories of surface lightness and illumination perception.

Ganglion cells have also been classified by the pattern and duration of their responses to changes in light their receptive fields (Enroth-Cugell66). *X cells* show a sustained response to increments or decrements in the centers of their receptive fields. *Y cells* show a brief transient change in response and then return to their base ring rate. X cells have small receptive fields, sum their inputs linearly, and produce signals that propagate at slow velocities along their axons. Y cells in contrast have relatively large receptive fields, sum their inputs in a non-linear fashion, and produce signals that travel along their axons at high velocities. Like the on-center/off-center subsystems histological and electrophysiological evidence for distinguishing between sustained and transient cells is strong, but it is not clear what impact this distinction has on visual experience.

Approximately 52% of retinal ganglion cells have receptive fields that show spectral as well as spatial opponency (Zrenner83). If a monochromatic stimulus is swept across the spectrum, at a particular wavelength the cell will change from a state of excitation to a state of inhibition (DeValois75). Some cells appear to take their input primarily from long and medium wavelength sensitive cones. These "red/green" opponent cells change state near 600nm. A much smaller proportion of color opponent cells appear to take their input from all three types of cones, with opposition between the sum of long and medium wavelength sensitive cones and short wavelength sensitive cones. These "yellow/blue" opponent cells change state close to 500nm. Both types of color opponent cells also exist in two forms. One form is inhibited at long wavelengths and excited at short wavelengths, and the other form shows the inverse pattern of response. The discovery of cells with spectrally opponent properties has been used to support physiologically based theories of color perception, most notably by Hurvich and Jameson (Hurvich81). As with the evidence for the on-center/off-center, and sustained/transient dichotomies also found in the response properties of retinal ganglion cells, it is important to recognize the kinds of coding of the patterns of light in the retinal image that happen in the eye, but what role this coding ultimately plays in visual perception is still an active research topic.

1.3 Visual pathways

1.3.1 The optic nerve

The long axons of the retinal ganglion cells form the *optic nerve*. The optic nerve consists of approximately one million fibers of which 100,000 serve receptors in the fovea. The optic nerve bundle exits the eyeball at the *optic disk*, approximately 17 degrees to the nasal side of the optic axis. There are no photoreceptors in this area commonly known as the blind spot. Normally we do not notice the absence of visual function in this area. This is consistent with clinical observations that stroke patients often do not notice scotomas in their visual fields. The means by which the visual system accomplishes this "filling-in" is still not completely understood.

1.3.2 The optic chiasm

The fibers of the optic nerve project to the optic chiasm. At this junction, fibers from the nasal portions of each retina cross over to the opposite side of the head. These crossing fibers join with fibers from the temporal portions of the opposite retina and project to the lateral geniculate nuclei (LGN) in each hemisphere. The LGN in the left hemisphere receives input from the temporal portion of the left eye and the nasal portion of the right eye. The converse situation holds for the LGN in the right hemisphere.

1.3.3 The lateral geniculate nuclei

Histological studies have shown that the LGN has a laminar structure. The six layers appear to receive specialized input from the optic nerve fibers of each eye. Layers 1, 4 and 6 receive input from the contralateral eye, layers, 2, 3, and 5 take input from the ipsilateral eye. Layers 1 and 2 are called the *magnocellular* layers. They are made up of large cells that take input primarily from the peripheral retina where non-spectrally opponent ganglion cells with large receptive fields and transient temporal characteristics are dominant. Layers 3 through 6 are called the *parvocellular* layers. The cells in these layers have small cell bodies that take input from the foveal region where spectrally-opponent cells with small receptive fields and sustained temporal characteristics are dominant. The striking differences in the functional properties of cells projecting to the magno- and parvo- cellular layers suggests that the eyes may in fact be serving two visual processing systems: a fast responding achromatic system very sensitive to motion but with low acuity; and a slow responding trichromatic system relatively insensitive to motion, but having high spatial acuity (Lennie84, Livingstone84).

1.4 The visual cortex

From the LGN fibers project to the *visual cortex* located in the posterior section of the brain. Primary visual cortex is known alternately as V1, area 17, and striate cortex. The cells in this area are organized into both layers and columns. Fibers from the LGN synapse in layer 4C. Magnocellular fibers project to layer 4α, parvocellular fibers project to layer 4β From here fibers project to layers 2, 3, and 4B before continuing to higher cortical areas. Livingstone and Hubel (Livingstone84) have done histological studies of these layers in monkeys and have found the following organization. Layers 2 and 3 consist of a mosaic of small regions they call *blobs*, the areas between the blobs are the *interblobs*. The interblobs receive input from the parvocellular layers, layer 4B receives input from the magnocellular layers, and the blobs receive input from both layers.

The blobs, interblobs and layer 4B have been found to have specific and distinct sensitivities. Blob cells are sensitive to the color or contrast of a stimulus, but not to its shape or motion. Interblob cells are selective for the orientation of an edge stimulus but are insensitive to its color and motion, and cells in layer 4B are selective for orientation and direction of motion but not color. Thus it appears that the functional specialization observed at the level of the LGN is also expressed and further refined in primary visual cortex.

At higher levels in visual processing, understanding of function becomes increasingly vague. Fibers from V1 project to *visual area 2* (V2). Histological analysis of V2 reveals three distinct patterns of cells: *thin stripes*, *thick stripes*, and *pale stripes*. Blobs project to the thin stripes which appear to be involved in color vision. Interblobs project to the pale stripes which seem to be processing aspects of form. The thick stripes receive input from layer 4B and are organized to process stereoscopic depth information.

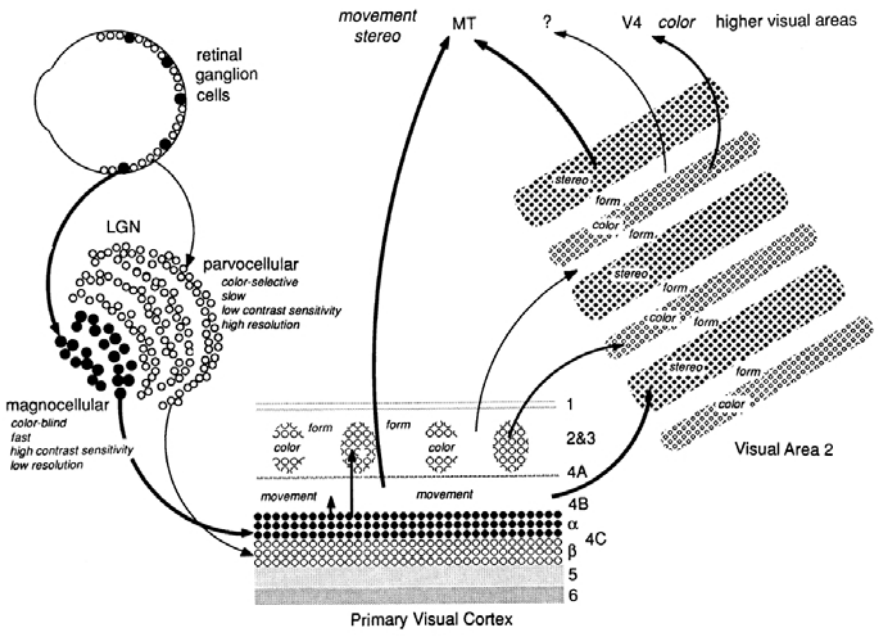

Figure 7: Cortical organization. From (Spillman91) after (Livingstone88).

From V2 the thin stripes project to *visual area 4* (V4) another area specialized for processing color information; the thick stripes project to *mediotemporal cortex* (MT) where motion and stereo information are processed; it is still unclear where projections from the pale stripes terminate.

The functional specificity observed at lower levels in vision continues at higher levels in visual processing. Cortex in the *temporal lobe* seems to be specialized for localization while the *parietal lobe* provides recognition functions. This has led to speculation that vision is divided into "where" and "what" systems. This conjecture is supported by case studies of stroke victims and cortical lesioning experiments on monkeys (Mishkin83) which show that brain damage can produce losses in one type of function without affecting the other.

2 The optical properties of the eye

2.1 Image formation in the eye

In the human eye, the cornea, iris, and lens comprise an optical system that forms an image on the retinal surface. As with any optical system, *abberations* in the optical components and *diffraction* effects produced by the entry aperture limit the resolution of the image. Resolution is a term that is used loosely in the computer graphics literature. Here it is close to its optical definition and means the fidelity with which object features are represented in an image. Features smaller than the resolution limit are not discernable in the image.

The image formed by the eye's optics falls on the photosensitive cells of the retina. The cells are arrayed in a roughly hexagonal grid. Cell density varies greatly with angle off the optic axis of the eye. A centrally located region known as the fovea has the highest cell density. Here cell centers have an angular separation of approximately 30 sec. (Osterberg35). The photosensitive cells sample the retinal image to produce a neural image representation. In terms of sampling theory, the spacing of the retinal photoreceptors is well matched to the optics of the eye. The filtering provided by the eye's optics allows the photoreceptors to create an accurate representation of the continuous retinal image through sampling at intervals given by the spacing of cells in the retinal mosaic (Snyder77).

The photosensitive cells in the retinal mosaic are interconnected into clusters known as receptive fields.

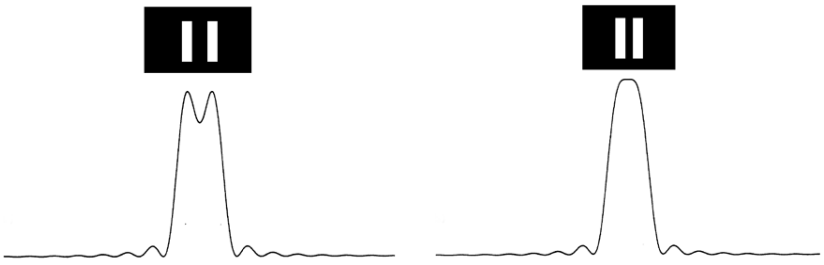

Figure 8: Limits of acuity due to the line spread function of the eye's optics.

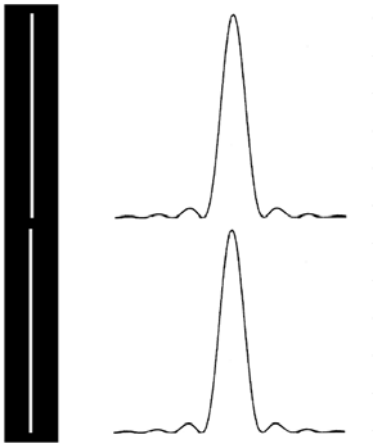

Figure 9: Limits of hyperacuity.

These receptive fields have an opponent organization with an excitatory central region and an inhibitory surround. Receptive fields vary greatly in size, being maximally sensitive to different scales of image features. The smallest receptive fields are in the fovea and are most sensitive to patterns with elements on the same scale as the spacing of foveal photoreceptors (Marr80).

These three factors, optical filtering, receptor sampling, and the receptive field organization of early visual processing determine the fidelity with which the visual system represents the patterns of light arriving at the eye. The perceptual measure of this fidelity is known as *visual acuity*.

2.2 Visual acuity

From a bright thin line in the visual field the eye's optics will produce a retinal image that has a slightly blurred intensity profile. If there are two bright lines side by side in the visual field, their retinal intensity profiles will overlap producing a composite intensity distribution with a central minimum. As the two lines are brought closer together the intensity of the central minimum will increase, reducing the contrast in this region of the image. The limiting distance necessary to allow these two points to be visually discriminated is a measure of the resolving power of the visual system. This is one measure of visual acuity. This example shows that acuity is a function of *contrast sensitivity*. The acuity limit is determined by the visual system's ability to detect the small contrast gradient in the center of the composite distribution. Contrast sensitivity limits this kind of visual acuity to approximately 30 seconds of visual angle (Thomas75).

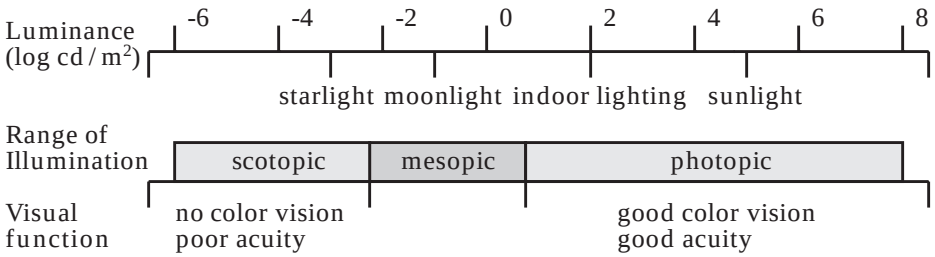

Figure 10: The range of luminances in the natural environment and associated visual parameters. After (Hood86).

2.3 Hyperacuity

There is another measure of visual acuity that is not a measure of resolution but instead specifies the visual system's ability to *localize* the positions of objects in the visual field. This is known as *vernier acuity*. If two bright lines are laid end to end, observers can detect misalignments of the lines as small as 4 to 6 sec. of visual angle (Westheimer77). This precision is remarkable in light of the fact that it corresponds to approximately one fifth of the distance between the foveal photoreceptors. While there is much speculation on how the visual system produces such a fine grained representation of position (Barlow79, Crick80, Watt83), what is clear is that this fine positional acuity must be based on information contained in the image representation produced by photoreceptor sampling of the optically filtered retinal image.

3 Light sensitivity and visual adaptation

The range of light energy we experience in the course of a day is vast. The light of the noonday sun can be as much as 100 million times more intense than starlight. Figure 10 shows the range of luminances we encounter in the natural environment and summarizes some visual parameters associated with this luminance range. Our visual system copes with this huge range of luminances by adapting to the prevailing conditions of illumination. Through *adaptation* the visual system functions over a luminance range of nearly 10 log units.

Adaptation is achieved through the coordinated action of mechanical, photochemical, and neural processes in the visual system. The pupil, the rod and cone systems, bleaching and regeneration of receptor photopigments, and changes in neural processing all play a role in visual adaptation.

Although adaptation provides visual function over a wide range of ambient illumination levels, this does not mean that we see equally well at all levels. For example, under dim illumination our eyes are very sensitive, and we are able to detect small differences in luminance, however our acuity for pattern details and our ability to distinguish colors are both poor. This is why it is difficult to read a newspaper at twilight or to correctly choose a pair of colored socks while dressing at dawn. Conversely, in daylight we have sharp color vision, but absolute sensitivity is low and luminance differences must be great for us to detect them. This is why it is impossible to see the stars against the sunlit sky.

Further, adaptation does not happen instantaneously. Nearly everyone has experienced the temporary blindness that occurs when you enter a dark theatre for a matinee. It can sometimes take a few minutes before you can see well enough to find an empty seat. Similarly, once you have dark adapted in the theatre and then go out into the daylight after the show, the brightness is at first dazzling and you need to squint or shield your eyes, but within about a minute, you can see normally again.

3.1 Physiological foundations of adaptation

Through adaptation the visual system functions over a luminance range of nearly 10 log units, despite the fact that the individual neural units that make up the system have a response range of only about 1.5 log units (Spillman90). Through four distinct adaptation mechanisms, the visual system moderates the effects of changing levels of illumination on visual response to provide sensitivity over a wide range of ambient light levels.

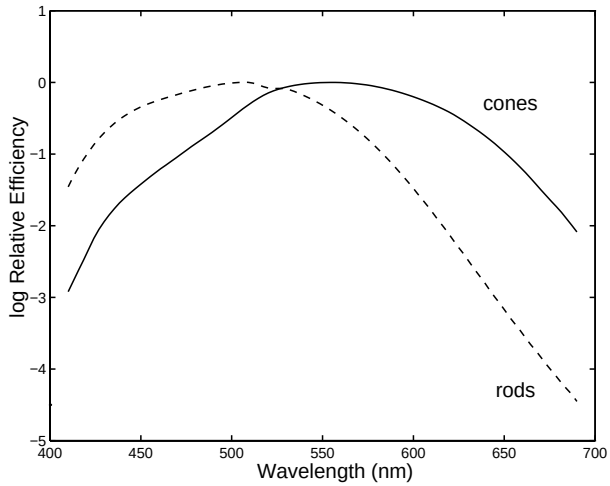

Figure 11: Scotopic V'_λ and photopic V_λ luminous efficiency functions. After (Wyszecki82).

3.1.1 The pupil

The most obvious mechanism available to regulate the amount of light stimulating the visual system is the pupil. Over a 10 log unit range of luminance, the pupil changes in diameter from approximately 7 mm down to about 2 mm (Pugh88). This range of variation produces a little more than a log unit change in retinal illuminance so pupillary action alone is not sufficient to completely account for visual adaptation (Spillman90). In fact, rather than playing a significant role in adaptation it is thought that variation in pupil size serves to mitigate the visual consequences of aberrations in the eye's optical system. At high levels where there is plenty of light to see by, the pupil stops down to limit the effects of the aberrations. At low levels where catching enough light to allow detection is more essential than optimizing the resolution of the retinal image, the pupil opens to allow more light into the eye.

3.1.2 The rod and cone systems

There are somewhere between 100-120 million rod and 7-8 million cone photoreceptors in each retina (Rigg71). The rods are extremely sensitive to light and provide achromatic vision at *scotopic* levels of illumination ranging from 10^{-6} to 10 cd/m^2. The cones are less sensitive than the rods, but provide color vision at *photopic* levels of illumination in the range of 0.01 to 10^8 cd/m^2. At light levels from 0.01 to 10 cd/m^2 both the rod and cone systems are active. This is known as the *mesopic* range. Relatively little is known about vision in the mesopic range but this is increasingly a topic of interest because computer-based office environments with CRT displays and subdued lighting exercise the visual system's mesopic range.

The rod and cone systems are not equally sensitive to light at all wavelengths. *Luminous efficiency functions* show how effective light of a particular wavelength is as a visual stimulus. Differences between the rod and cone systems lead to separate photopic and scotopic luminous efficiency functions that apply to typical daytime and nighttime illumination levels. Figure 11 shows the normalized scotopic and photopic luminous efficiency functions developed by the CIE (Wyszecki82).

3.1.3 Bleaching and regeneration of photopigments

At high light intensities, the action of light depletes the photosensitive pigments in the rods and cones at a faster rate than chemical processes can restore them. This makes the receptors less sensitive to light. This process is known as *pigment bleaching*. Early theories of adaptation were based the idea that light adaptation was produced by pigment bleaching and dark adaptation was produced by pigment restoration (Hecht34). However pigment bleaching cannot completely account for adaptation for two reasons: first, a substantial amount of adaptation takes place in both the rod and cone systems at ambient levels where little bleaching

occurs (Granit39); and second, the time courses of the early phases of dark and light adaptation are too rapid to be explained by photochemical processes alone (Crawford47).

3.1.4 Neural processes

The neural response produced by a photoreceptor cell depends on chemical reactions produced by the action of light on the cell's photopigments. The cell's response to light is limited by the maximum rate and intensity of these chemical reactions. If the reactions are occurring near their maximum levels, and the amount of light striking the photopigments is increased, the cell may not be able to fully signal the increase. This situation is known as *saturation*. The result of saturation is *response compression*: above a certain level incremental increases in light intensity will produce smaller and smaller changes in the cell's response rate.

The rod and cone photoreceptors connect through a network of neurons in the retina to ganglion cells whose axons form the optic nerve. Adaptive processes sited in this neural network adjust the base activity and gain of the early visual system to mitigate the effects of response compression in the photoreceptors. A *multiplicative process* adjusts the gain of the system by effectively scaling the input by a constant related to the background luminance. This process acts very rapidly and accounts for changes in sensitivity over the first few seconds of adaptation. A slower acting *subtractive process* reduces the base level of activity in the system caused by a constant background. This process accounts for the slow improvement in sensitivity measured over minutes of adaptation (Adelson 1982).

3.2 Psychophysics of adaptation

The physiological mechanisms described above provide the basis for visual adaptation. The action of these mechanisms is reflected in the changes in visibility, color appearance, visual acuity, and sensitivity over time that can be observed in everyday experience and measured in psychophysical experiments.

3.2.1 Threshold studies

For an object to be visible, the light coming from that object must be transduced into electrochemical signals in the visual nervous system. The transduction process depends upon light energy activating pigment molecules in the outer segments of the rod and cone photoreceptors. The efficiency of this transduction process is the earliest factor that limits visual sensitivity. In a classic psychophysical study, Hecht (1942) calculated that human rods are sensitive enough to signal the absorption of single photons.

Although this study showed that physiological changes in the visual system can be measured from the absorption of a single photon by a rod, higher levels of neural activity are necessary before a stimulus is perceptible. Hecht showed that absorptions in somewhere between 5 and 14 rods in a region 10' in diameter must be registered within 1 ms for a stimulus to be seen.

Visual sensitivity is often measured psychophysically in a *detection threshold* experiment. In the typical experimental paradigm, an observer is seated in front of a blank screen that fills their field of view. To determine the absolute threshold the screen is made dark. To determine the contrast threshold a large region of the screen is illuminated to a particular background luminance level. Before testing begins, the observer fixates the center of the screen until they are completely adapted to the background level. On each trial a disk of light is flashed near the center of fixation for a few hundred milliseconds. The observer reports whether they see the disk or not. If the disk is not seen its intensity is increased on the next trial. If it is seen, its intensity is decreased. In this way, the detection threshold for the target disk against the background is measured.

3.2.2 Changes in threshold sensitivity

As the luminance of the background in a detection threshold experiment is increased from zero, the luminance difference between target and background required for detection increases in direct proportion to the background luminance. Plotting the detection threshold against the corresponding background luminance gives a *threshold-versus-intensity (t.v.i.)* function. Figure 12 shows the psychophysically measured t.v.i. functions for the rod and cone systems.

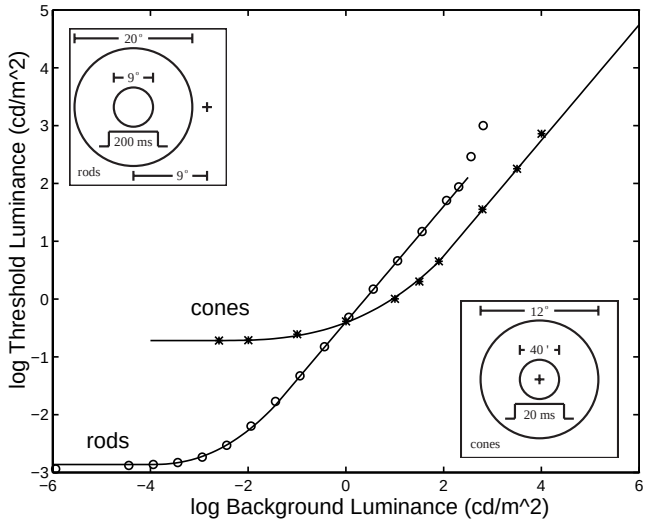

Figure 12: A psychophysical model of detection thresholds over the full range of vision.

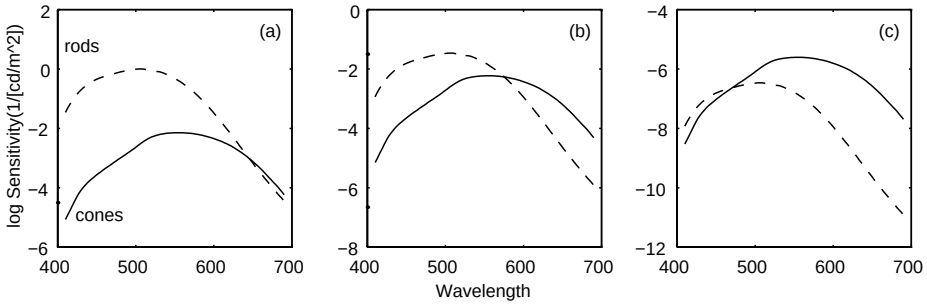

Figure 13: Changes in the spectral sensitivity of the visual system at (a) scotopic, (b) mesopic, and (c) photopic illumination levels. After Hood (1986).

At luminance levels below about -4 log cd/m^2, the rod curve flattens to a horizontal asymptote. This indicates that the luminance of the background has little effect on the threshold which approaches the limit for detecting a stimulus in the dark. At levels above 2 log cd/m^2 the curve approaches a vertical asymptote. This indicates that the rod system is being overloaded by the background luminance with the result that no amount of luminance difference between the background and target will allow detection.

Over a wide middle range covering 3.5 log units of background luminance the function is linear, this relationship can be described by the function $\Delta L = kL$. This relationship is known as *Weber's law* (Riggs71). Weber's law behavior is indicative of a system that has constant contrast sensitivity, since the proportional increase in threshold with increasing background luminance corresponds to a luminance pattern with constant contrast.

The other curve in Figure 12 shows the t.v.i. function for the cone system. In many ways the rod and cones show similar patterns of response. At levels below -2.6 log cd/m^2, the t.v.i function is essentially flat indicating that the background has no effect on the response threshold. In this region the cones are operating at their absolute levels of sensitivity. At background levels above 2 log cd/m^2 the function is linear, indicating Weber's law behavior and constant contrast sensitivity. One important difference between the rod and cone functions is that the cone system never saturates in the upper reaches of the luminance range. Instead, pigment bleaching gradually lowers sensitivity all the way up to damaging intensity levels.

The rod and cone t.v.i. functions can be placed on the same graph to show the relative sensitivities of the systems and to show how threshold sensitivity varies over a wide range of scotopic and photopic background luminances. At background luminances from about -6 to 0 log cd/m^2 the rod system is more sensitive than the cone system. In this range the rods account for the magnitude of the detection threshold.

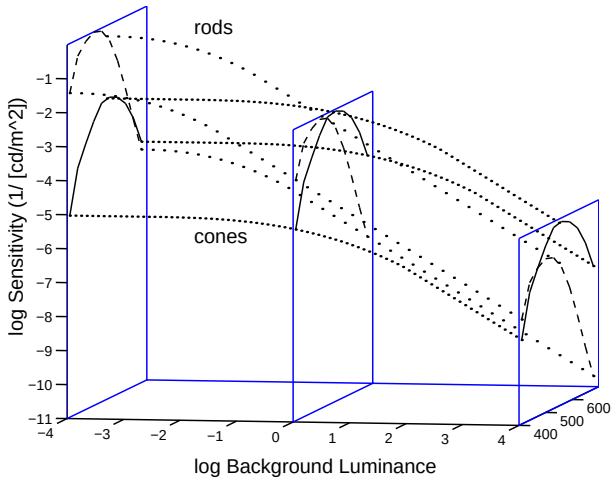

Figure 14: A model of threshold sensitivity as a function of wavelength and background luminance for the rod and cone systems.

As the background luminance is increased, the rod system loses sensitivity and the detection threshold rises. At a background level around 0 log cd/m^2 the rod and cone t.v.i. functions cross. Above this level the cone system is more sensitive than the rod system and it accounts for the detection threshold. Over a wide range of background luminances the visual system's threshold sensitivity can be described by the envelope of the rod and cone t.v.i. curves.

3.2.3 Changes in color appearance

The spectral sensitivities of the rod and cone systems are described by the scotopic and photopic luminous efficiency functions. When presented graphically, the functions are typically normalized which masks the fact that the rod and cone systems differ greatly in sensitivity and operate over different luminance ranges.

Figure 13 (a) shows the visual system's spectral sensitivity at scotopic levels. At these levels detection is dominated by the rod system. Absolute sensitivity is quite high, but since the rod system is achromatic, color will not be apparent.

Figure 13 (b) shows spectral sensitivity at mesopic levels. Here the rod and cone systems are nearly equal in absolute sensitivity. Detection at a particular wavelength will be served by the more sensitive system. The graph shows that the rods will detect wavelengths below about 575 nm and the cones will detect wavelengths above this point.

Figure 13 (c) shows the visual system's spectral sensitivity at photopic levels. At these levels detection is dominated by the cone system. Absolute sensitivity has dropped considerably, but due to the trichromatic nature of the cone system, colors will now be seen.

Figure 14 shows the luminous efficiency functions as surfaces positioned with respect to the rod and cone system threshold sensitivities at different luminance levels. This 3d graph shows how the visual system's spectral sensitivity changes with changing luminance levels and which system is dominant at a particular level. The subfigures show cross sections of these spectral sensitivity vs. luminance surfaces.

This model of the changes in spectral sensitivity with changing luminance levels can account for a number of different color appearance phenomena observed over the scotopic to photopic range. First, at low luminance levels vision will be achromatic since detection at all wavelengths is served by the rod system. As the luminance level is raised into the mesopic range, the cone system will become active and colors will begin to be seen beginning with the long wavelength reds and progressing toward the middle wavelength greens. Only at relatively high luminances will short wavelength blue targets begin to appear colored.

3.2.4 Changes in visual acuity

Acuity is a measure of the visual system's ability to resolve spatial detail. Acuity is often measured clinically

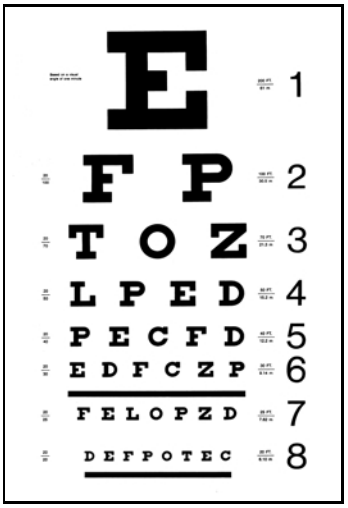

Figure 15: The Snellen acuity chart.

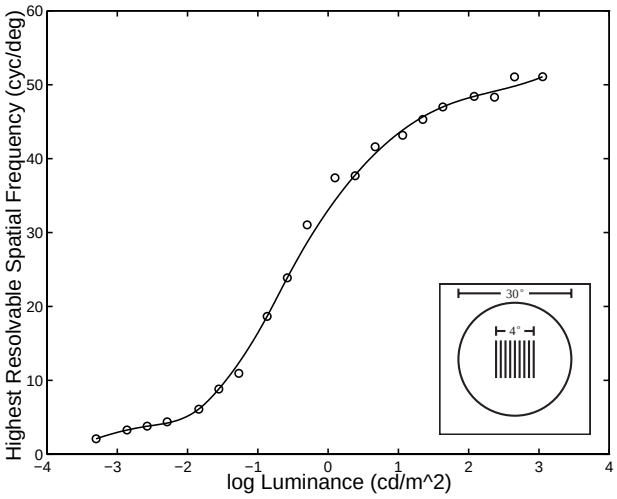

Figure 16: Changes in grating acuity as a function of background luminance. After Shaler (1937).

with the Snellen chart. A portion of the Snellen chart is shown in Figure 15. The letters of the chart are constructed such that the strokes of each character subtend precise visual angles when viewed from a distance of 20 feet. The bottom line of the chart is taken as the standard of normal acuity. At 20 feet each character stroke in the bottom line (8) subtends one minute of visual angle. A viewer who can correctly identify the characters on this line is said to have 20/20 vision. The upper lines in the chart have progressively wider stroke widths. These lines are used to assess subnormal acuity. For example each stroke in the characters on line 5 is twice as big as those on line 8. A person with normal acuity can identify the characters in this line from a distance of 40 feet. If you can just identify this line at the standard 20 foot viewing distance then you have 20/40 vision. The large E on line 1 of the chart is equivalent to a visual acuity of 20/200.

Acuity is lower at scotopic levels of illumination than at photopic levels. The curve in Figure 16 shows how visual acuity changes with background luminance. The data cover the range from daylight down to starlight. The experiment measured acuity by testing the detectability of square wave gratings of different spatial frequencies. The graph shows that the highest frequency grating that can be resolved drops from a high of about 50 cycles/degree at 3 log cd/m^2 down to about 2 cycles/degree at -3.3 log cd/m^2. This is equivalent to a change from almost 20/10 vision at daylight levels down to nearly 20/300 under starlight. This curve can be used to predict the visibility of scene details at different levels of illumination. At low levels of illumination it should be difficult to resolve detailed patterns, like the smaller lines on the Snellen

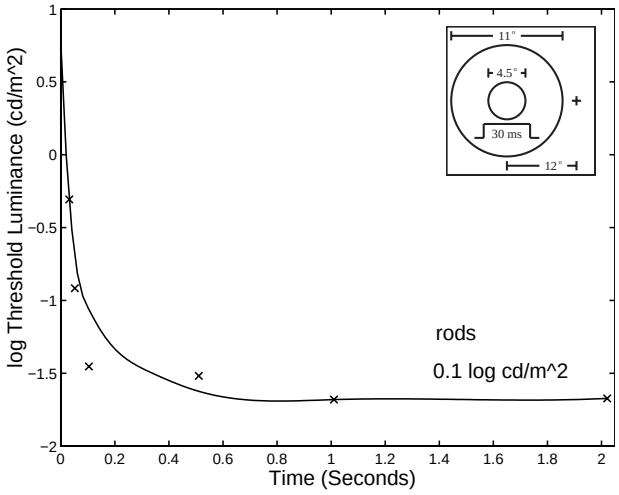

Figure 17: The time course of light adaptation in the rod system. After (Adelson82).

chart or fine textures.

3.2.5 The time-course of adaptation

Adaptation does not happen instantaneously. If you are seated in a dark room and the lights are suddenly switched on it takes several seconds before you adjust to seeing at the new level of illumination. This process is known as *light adaptation*. Figure 17 shows the results of an experiment on the time course of light adaptation in the rod system (Adelson82). Prior to the experiment the observer was dark adapted. At the beginning of the experiment a large background field of 0.5 log cd/m^2 was switched on and from that moment forward the threshold was measured repeatedly. In the moment after the background field was switched on the detection threshold jumped from its dark adapted level to about -0.25 log cd/m^2, but after 2 seconds the threshold has dropped back to about -1.7 log cd/m^2. The graph shows that light adaptation in the scotopic range of the rod system is extremely rapid. More than 80% of sensitivity recovery occurs within the first 2 seconds, and nearly 75% happens within the first 200 ms.

Figure 18 shows the results of a similar experiment on the time-course of light adaptation in the cone system (Baker49). As with the rod system, thresholds are highest immediately after the onset of the background field. At a 3.75 log cd/m^2 background level, the instantaneous threshold is about 3.5 log cd/m^2. The threshold decreases over time and reaches a minimum after about 3 minutes of exposure. The threshold drops more than 0.5 log units during this period. After 3 minutes the threshold rises again slightly (due to interactions between neural and photochemical processes in adaptation) and reaches its fully adapted level at about 10 minutes. This experiment also shows that the time course of light adaptation in the cone system is slower than the rod system.

Visually, light adaptation provides a distinctive experience. When we go quickly from low to high levels of illumination, at first everything is painfully glaring and we squint or close one eye to reduce the discomfort. However over time the overall brightness of the visual field diminishes to more comfortable levels and normal vision is restored.

Figure 19 shows the time-course of *dark adaptation* as measured by Hecht (1934). In this experiment, the observer was first adapted to a high background luminance and then plunged into darkness. Detection thresholds were measured continuously over more than 30 minutes. The graph shows the detection threshold as a function of time in the dark. The kinked threshold curve is actually the envelope of the curves for the separately tested rod and cone systems. In the first 5 minutes after the adapting field is switched off, the threshold drops rapidly, but then it levels off at a relatively high level because the cone system has reached its greatest sensitivity, but the rod system has still not recovered significantly. After about 7 minutes rod system sensitivity surpasses that of the cone system and the threshold begins to drop again. This point is known as the *Purkinje break* (Riggs71) and indicates the transition from detection by the cone system to

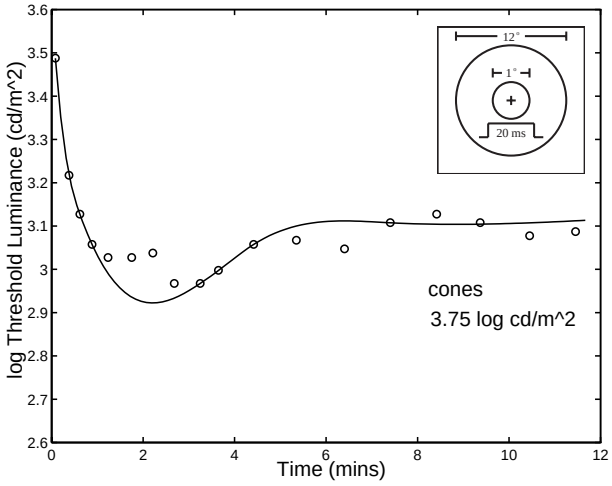

Figure 18: The time course of light adaptation in the cone system. After (Baker49).

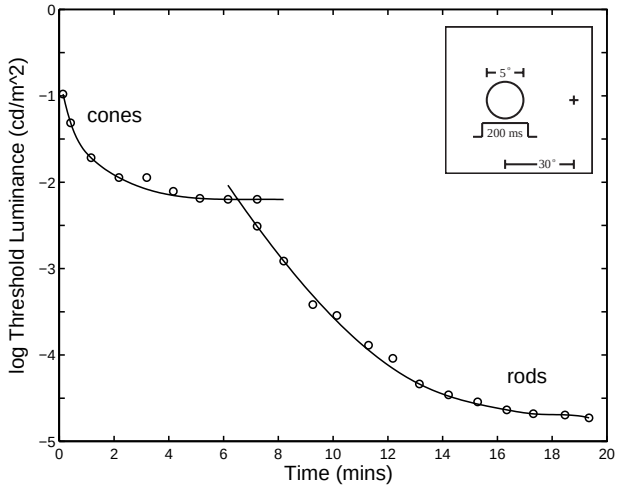

Figure 19: The time course of dark adaptation. After Riggs (1971).

detection by the rods. Changes in the threshold can be measured out to about 35 minutes, at which point the visual system has reached its absolute levels of sensitivity, and the threshold has dropped nearly 4 log units.

Visually, dark adaptation is experienced as the temporary blindness that occurs when we go rapidly from photopic to scotopic levels of illumination. The relatively slow time-course of dark adaptation means that vision can be impaired for several minutes when we move quickly from high illumination levels to low ones.

3.3 Summary

The cumulative achievement of adaptation is that the visual system is sensitive over a vast range of ambient light levels despite severe limits on the dynamic ranges of the individual neural units that make up the system. However this does not mean that we see equally well at all levels of illumination. The experimental results show that threshold visibility, color appearance, and visual acuity are different at different illumination levels, and that these visual parameters change over the time-course of light and dark adaptation.

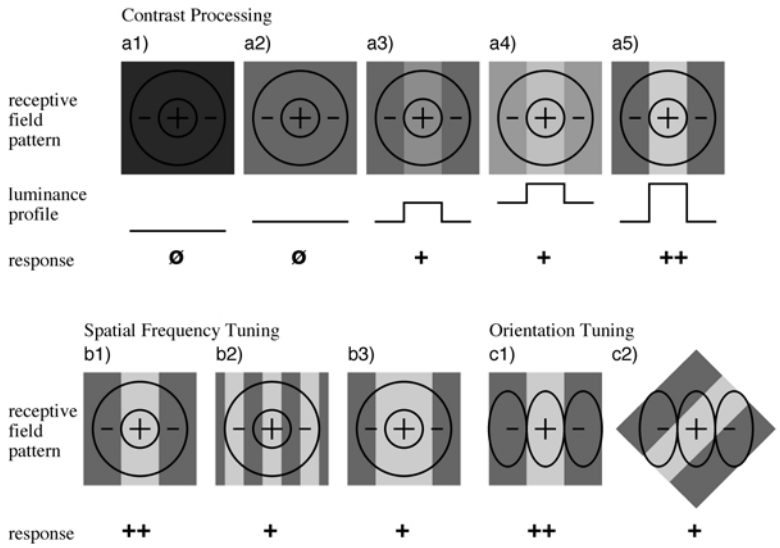

Figure 20: Properties of visual system receptive fields: (a) contrast processing; (b) spatial frequency tuning; (c) orientation tuning.

4 Seeing spatial patterns

We see on the basis of the patterns of light projected onto our retinas by objects and surfaces in the visual field. The variations in the color and intensity of light in these retinal patterns are essential for visual perception. If we eliminate these patterns by uniformly illuminating the retina we may have a sensation of light, but we won't "see" anything in particular and our perceptual experience will be amorphous.

Spatial vision is the field of psychology that studies of how patterns of light on the retina are interpreted by the visual system. The goal of the research in spatial vision is to understand the visual mechanisms that transform the patterns of light in the retinal image into the colors, sizes, shapes, locations, and motions of the three-dimensional objects we perceive in the world around us. The field has a long tradition which draws on both *physiological* studies of the electrical responses of cells in the visual pathways of primates and lower animals, as well as on *psychophysical* studies of the responses of human observers to simple visual stimuli.

4.1 Physiological foundations of spatial vision

One of the most fundamental findings in the field of spatial vision is that the rod and cone photoreceptors which transduce light into electrical impulses in our nerve fibers are not independent of one another but interact in various ways. Figure 2 shows a diagram of a cross section through the retina. Amacrine, bipolar, and horizontal cells form neural networks in the plexiform layers of the retina that synapse on ganglion cells whose axons make up the optic nerve.

4.1.1 Receptive fields

To understand the properties of these neural networks, Kuffler (1953) made electrophysiological measurements of the responses of retinal ganglion cells in the cat. He found that each ganglion cell took its input from a spatially localized region of the retina called its *receptive field*.

Kuffler found that these receptive fields had a characteristic center/surround organization with antagonism between the center and surround. Center/surround antagonism in receptive fields results in ganglion cells that respond primarily to contrast rather than to simple light intensity. This is illustrated in Figure 20a which shows the response of an idealized ganglion cell to various types of stimuli. In the dark, (Figure 20a1) the ganglion cell fires spontaneously at its base rate. If the intensity of light falling on the ganglion cell's receptive field is raised uniformly, (Figure 20a2) the excitatory and inhibitory regions of the field cancel and

the cell continues to fire at its base rate. If however, a bar pattern is introduced with contrast between the bar and the background (Figure 20a3), the excitation produced by the center will exceed the inhibition produced by the surround and the cell will increase its firing rate. Figures 20a4 and 20a5 show that the cell's response depends upon the contrast of the pattern rather than it's absolute intensity. In Figure 20a4 the luminance of the bar and background have both increased, but the cell continues to give the same response. However when the contrast between the bar and background is increased, (Figure 20a5) the response goes up as well.

Researchers have also found that different ganglion cells have receptive fields of different sizes and that these receptive fields overlap in the retina so that at any retinal location receptive fields of many sizes can be found. Different sized receptive fields result in ganglion cells that are selectively responsive to patterns of different scales.

4.1.2 Spatial tuning

Enroth-Cugell and Robson (1966) measured the response properties of retinal ganglion cells in the cat to sinusoidal grating patterns of different spatial frequencies. They found that the cells responded to limited ranges of spatial frequencies related to the sizes of their receptive fields. This spatial frequency selectivity of ganglion cell receptive fields is illustrated in Figure 20b.

The receptive field of the idealized ganglion cell has an excitatory center and inhibitory surround. If the receptive field is illuminated with the grating pattern shown in Figure 20b1 where the spatial frequency of the grating is such that the bars match the widths of the center and surround, there will be significant excitation from the center and not much inhibition from the surround so the cell will respond near its maximum rate. If however, we raise or lower the grating's spatial frequency as shown in Figures 20b2 and 20b3 there may be both less excitation from the center, and more inhibition from the surround so the cell will respond at a lower rate. The *spatial frequency tuning* of a cell depends upon the size of its receptive field. Cells with small receptive fields will respond to high ranges of spatial frequencies. Cells with larger fields will respond to lower ranges.

Although early studies focused on the response properties of cells in the retina, as more sophisticated electrophysiological techniques became available researchers began to investigate higher levels in the visual system including the visual cortex. These studies found that the receptive field organization first seen in the retina is in evidence throughout the visual system.

4.1.3 Orientation tuning

Hubel and Wiesel (1962,1968) did electrophysiological studies of cells in the visual cortex of the cat and monkey, mapping the properties of cortical receptive fields. At this level of the visual system cells show greater selectivity for specific features of visual patterns. For example Hubel and Weisel found cells that respond to edges rather than bars, showing selectivity for pattern symmetry. They also found cells that respond to motion in one direction but not in the other bringing this selectivity to the temporal domain. One characteristic that many cells showed was selectivity for orientation. They found that many cells responded maximally to patterns at a particular orientation and that response declined rapidly as the pattern was tilted away in either direction. Orientation selectivity in cortical cells is illustrated in Figure 20c.

Figure 20c1 shows an idealized receptive field for a cortical cell. The receptive field still shows an antagonistic center surround organization, but the field is elongated in a particular direction. This elongation of the field accounts for the cell's orientation selectivity. If a grating pattern of the right spatial frequency and orientation stimulates the cell's receptive field then there will be significant excitation and little inhibition and the cell will respond maximally. However, if the orientation of the grating is changed as in Figure 20c2 then there will be a mix of excitation and inhibition and the response will be reduced. Thus the cell exhibits *orientation tuning*.

The results of physiological studies of the retina and cortex in cats and primates reveal much of the functional organization of early visual processing. The experiments described have shown that the light patterns in the retinal image produced by objects in the visual field are represented as a set of responses in visual mechanisms that are selective for contrast, spatial frequency, and orientation. The coded responses of these mechanisms (along with others that represent color, motion, binocular disparity, etc.) are the fundamental building blocks of perceptual experience.

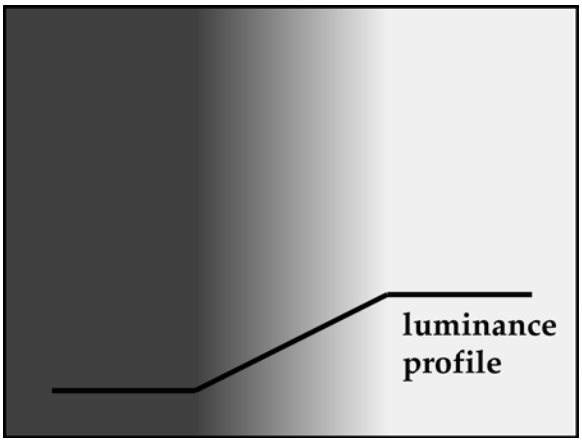

Figure 21: Mach bands: Two regions of differing but uniform luminance are joined by a linear luminance ramp. At the transition from the dark region to the ramp, an even darker vertical bar is seen. At the transition from the ramp to the light region an even lighter vertical bar is seen. These dark and light bars are not in the image. They provide direct evidence for lateral interactions in visual processing.

Although the results of these experiments provide valuable information about visual structures and mechanisms, to fully understand *human* vision, another approach must be taken because except in limited clinical settings it is not possible to conduct physiological studies of human beings. *Visual psychophysics* is the quantitative study of the relationship between visual stimuli and perceptual responses. Experimental findings in visual psychophysics complement the results of physiological studies and provide a more complete picture of the relationships between visual stimulation and perceptual experience.

4.2 Psychophysics of Spatial Vision

Given the physiological evidence for visual mechanisms in animals selective for contrast, spatial frequency, and orientation, psychophysicists began to test for the existence of similar mechanisms in human vision.

4.2.1 Contrast processing in receptive fields

The psychophysical evidence for contrast processing mechanisms in human vision has a long history going back as far as Mach (Ratliff65) who suggested that *lateral inhibition* could account for the bright and dark Mach bands seen at discontinuities in luminance profiles, and Hering who proposed in his *opponent process theory* that antagonism between visual mechanisms was a fundamental principle of color and lightness perception and could explain such visual phenomena as simultaneous contrast and color constancy (see (Hurvich81) for a review). Modern psychophysical evidence for these mechanisms comes from the work of Campbell and Robson (1968) who measured the *contrast sensitivity function* of human vision for sine wave gratings of different spatial frequencies.

Campell and Robson tested contrast thresholds for sine wave gratings over a range of spatial frequencies and plotted the contrast sensitivity function shown in Figure 23a. In the fovea, at the luminance level tested, contrast sensitivity peaks for a pattern of 4-5 cycles/degree where a contrast of 0.5% can be detected. The graph shows that threshold contrast sensitivity declines for both higher and lower spatial frequencies. At high spatial frequencies the decline in sensitivity closely follows losses in physical image contrast due to limitations in the eye's optics At low spatial frequencies the decline can be at least partly explained by the limits on the sizes of the largest receptive fields.

4.2.2 Spatial frequency tuning

As was shown in the previous section, the receptive field organization of visual processing in cats and primates leads to visual mechanisms that are tuned to different ranges of spatial frequencies. Blakemore and Campbell

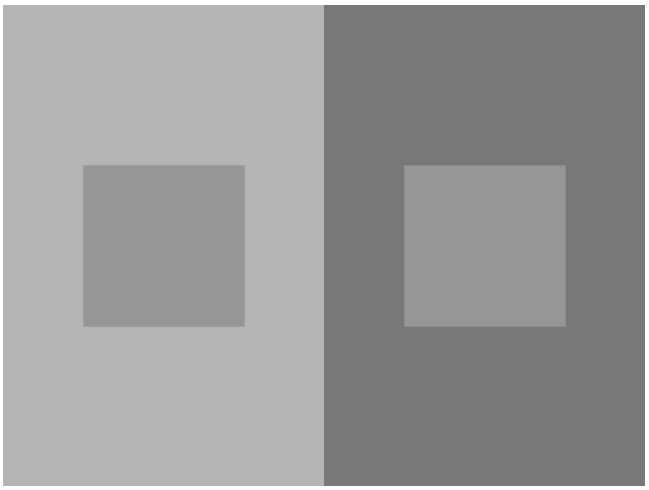

Figure 22: Simultaneous contrast: a middle gray target seen against a light gray surround will appear darker than the same gray target seen against a dark gray surround. The differences in appearance are due to antagonistic interactions between the neural signals produced by different regions of the retina. Simultaneous contrast can be viewed as a process of *induction* (Hurvich81). Where the positive neural activity produced by the light background induces a negative response in the target region that is summed with the activity produced by the target itself. This results in the apparent darkening of the target on the light surround. Similar reasoning can be applied to explain the apparent lightening of the gray target on the dark surround.

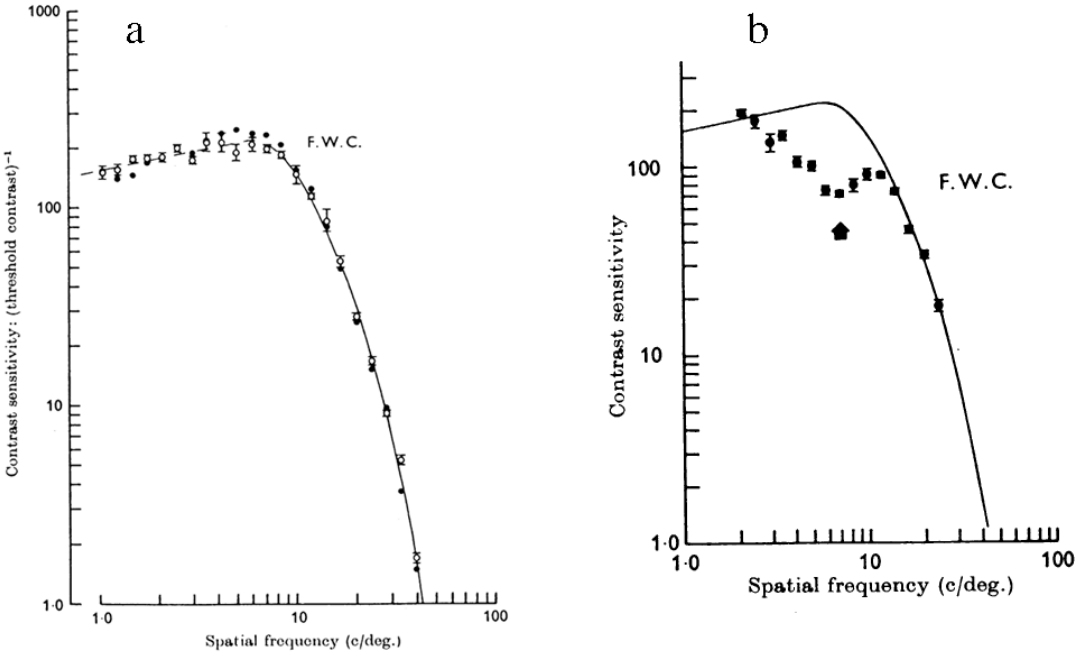

Figure 23: (a) The contrast sensitivity function of subject F.W.C.: Patterns were sine-wave gratings. Mean luminance of the gratings was 100 cd/m^2. Contrast sensitivity is plotted on an arbitrary logarithmic scale against spatial frequency. Filled and open symbols show two independent measurements on the same subject. (b) Contrast sensitivity function for F.W.C. after adaptation to a sine-wave grating of 7.1 cpd. Note the depression in sensitivity in the spatial frequency band near the adapting frequency. From (Blakemore69).

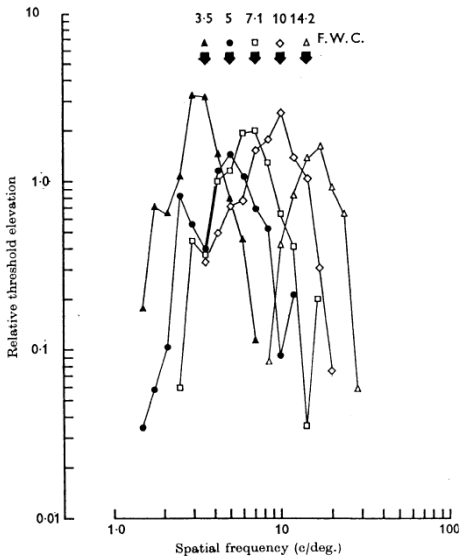

Figure 24: Spatial frequency tuning in human visual mechanisms: Curves show the relative elevation in contrast thresholds caused by adaptation to sine-wave gratings of various frequencies. Each arrow shows an adapting frequency and the symbol above it indicates the corresponding threshold elevation curve. Note the frequency-tuned nature of the threshold elevation effects. From (Blakemore69).

(1969) conducted a series of psychophysical experiments to see if frequency tuned mechanisms exist in human vision.

They used an *adaptation* paradigm in their experiments. Prior to the experiment they measured the subject's contrast sensitivity function. They then had the subject inspect a grating pattern of a particular spatial frequency for one minute, instructing the subject to move their eyes constantly to avoid afterimages. They then re-measured the subject's contrast sensitivity function. Their results are shown in Figure 23b.

Contrast sensitivity is depressed for spatial frequencies close to the adapting frequency. The loss of sensitivity is greatest at the adapting frequency, but sensitivity is also depressed for spatial frequencies within a 2 octave band around the adapting frequency. Frequencies outside of this range are unaffected.

Blakemore and Campbell repeated the adaptation experiment at a number of different spatial frequencies and found a similar pattern of results in each case. The results are summarized in Figure 24. Each curve shows the relative *threshold elevation* (1/loss in sensitivity) caused by adaptation to a grating of a particular spatial frequency. The curves are all similar in shape: the peak threshold elevation occurs at the adapting frequency. Spatial frequencies in a band near the adapting frequency are affected, but contrast sensitivity for spatial frequencies outside these bands is normal. A visual demonstration of spatial frequency tuning in human vision is presented in Figure 26a.

Wilson and Gelb (1984) performed a set of related experiments on spatial frequency discrimination to estimate the spatial frequency tuning of visual mechanisms in the fovea. Drawing inspiration from line-element models of color discrimination (Stiles78), they proposed a *multiple mechanism* model to account for their data on spatial frequency discrimination. The model illustrated in Figure 25 has six spatial frequency tuned mechanisms with different peak frequencies and spatial bandwidths. The number of mechanisms in the model and the tuning parameters of each mechanism were derived by fitting the experimental data and so provide a good account of actual visual performance.

While there is ongoing debate about the number, peak frequencies, and bandwidths of spatially tuned mechanisms in human vision, the general form of the results presented by Blakemore and Campbell and Wilson and Gelb have been corroborated in numerous subsequent experiments (see (Wilson91) for a review). These results provide strong psychophysical evidence for spatial frequency tuned mechanisms in human vision. Though we cannot pinpoint the particular physiological locus of these tuned mechanisms in the human visual system, the experiments show that their influence can be measured by concrete changes in our perceptual performance.

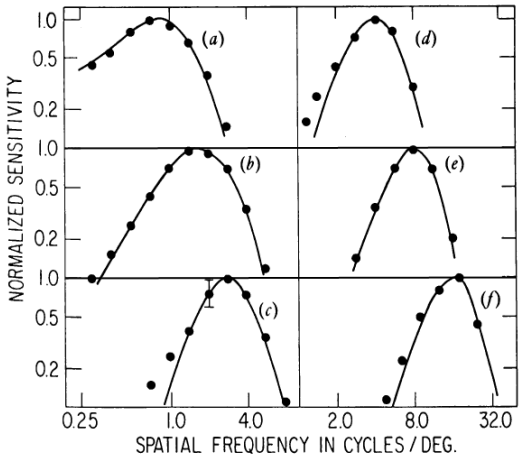

Figure 25: Model of spatial frequency tuned mechanisms in the human visual system: Points show mean data from three subjects on the spatial frequency tuning of six visual mechanisms. The curves show difference-of-Gaussian (DOG) function fits to the data for each mechanism. Mechanisms a-f are arranged in order of increasing peak spatial frequency. Each curve is plotted on a normalized sensitivity scale. Note that the spatial frequency scales in the right and left halves of the figure are different. From (Wilson84).

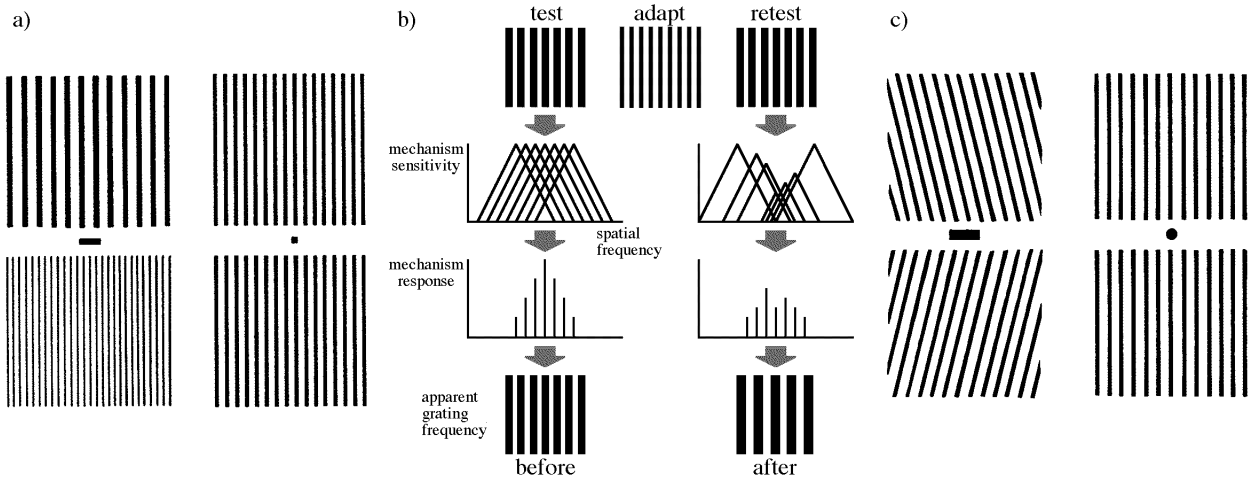

Figure 26: Demonstration of spatial frequency and orientation specific aftereffects due to adaptation. In (a) the grating pair on the right have the same spatial frequency. The grating pair on the left have higher and lower spatial frequencies. After adaptation to the left-hand pair (by scanning the central fixation bar for about 1 minute), the right hand pair will appear to have different spatial frequencies when the central spot is fixated. This aftereffect causes a shift in the apparent frequency of the test grating away from the frequency of the adapting grating. Thus after adaptation, the top grating of the right pair will appear to have a higher frequency and bottom grating will appear to have a lower frequency. This aftereffect can be explained by the illustration in (b). Perception of a grating pattern is mediated by a number of spatial frequency tuned mechanisms. The appearance of the grating is determined by the combined responses of the different mechanisms. Adaptation to a grating with a particular frequency depresses the response of mechanisms sensitive to that frequency. After adaptation, viewing the original grating now causes a biased pattern of responses in the mechanisms that results in the apparent frequency shift. A similar orientation-specific aftereffect can be seen in (c). Inspection of the tilted grating patterns on the left for approximately 1 minute will cause the vertical gratings on the right to appear to be tilted in the opposite direction. (a) After (Blakemore69) ; (b) after (Braddick78); (c) after (Schiffman82).

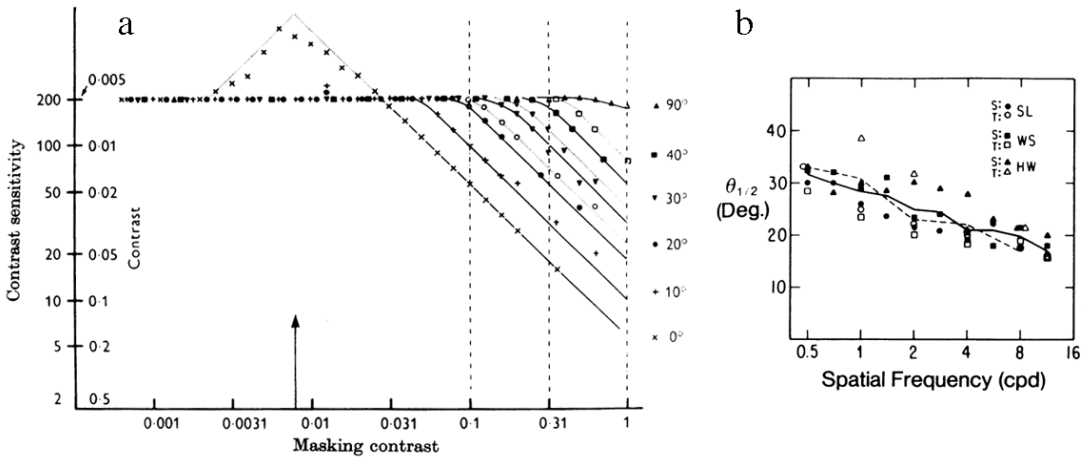

Figure 27: (a) Orientation tuned mechanisms in the human visual system: Curves show contrast sensitivity for a vertical sine-wave test grating as a function of the contrast of a masking grating. At low contrasts the mask has little effect on contrast sensitivity. At higher mask contrasts contrast sensitivity falls in proportion to the contrast of the masking grating. Individual curves show how the orientation of the masking grating modulates the masking effect. Note that the magnitude of masking diminishes with the angular difference between the masking and test gratings. The anomalous data seen at low contrasts of the 0° masker is a *facilitation* effect that will be described in a later section. From (Campbell66). (b) Bandwidth estimates of orientation-tuned mechanisms in the human visual system. The data shows the 50% amplitude, half-bandwidths of orientation-tuned visual mechanisms at different spatial frequencies. Different symbols are used for each of the three subjects. The filled symbols are for sustained presentations. The open symbols are for transient presentations. The solid line runs through the average half-bandwidth value at each spatial frequency. The dashed line compares these results to physiological data from primates (DeValois82). Note that the orientation bandwidths of the mechanisms become progressively narrower with increasing spatial frequency. From (Phillips84).

4.2.3 Orientation tuning

A similar pattern of results can be found from psychophysical experiments testing the orientation tuning of mechanisms in human vision. Campbell and Kulikowski (1966) used a *masking* paradigm to measure contrast sensitivity for a test grating in a vertical orientation, superimposed on a background grating which varied in orientation. Their results are shown in Figure 27a.

When the test and background gratings have the same orientation (indicated by the x's in the 0° curve) sensitivity for the test grating drops in direct proportion to the suprathreshold contrast of the background grating. The apparent enhancement in sensitivity at low background contrasts is a *facilitation* effect that will be described in the following section on visual masking.

When the test and background gratings have different orientations, the drop in contrast sensitivity is a function of the angle between the gratings. The greater the angle between the gratings the less effect the background grating has on sensitivity for the test grating. This is indicated by the parallel curves in Figure 27a which show that as the angle between the gratings is increased, higher and higher background contrasts are needed to produce the same reduction in contrast sensitivity. Campbell and Kulikowski found that the magnitude of the effect was reduced by a factor of 2 when the gratings differ by 12°. which they took to indicate that the visual mechanism they tested has an orientation tuning of approximately 24°. Figure 26c presents a visual demonstration of orientation tuning in human vision.

Phillips and Wilson (1984) performed a related set of experiments to determine the orientation tuning of human visual mechanisms at different spatial frequencies. The test pattern was a spatially localized grating patch superimposed upon a background grating that varied in orientation. Figure 27 shows the orientation tuning half-bandwidths of the visual mechanisms at different spatial frequencies. These half-bandwidths were estimated from threshold elevation experiments similar to Campbell and Kulikowski's. The results show that the visual system is more tightly tuned to orientation at high spatial frequencies than at low spatial frequencies. The graph shows that at a spatial frequency of 0.5 cycles/degree the orientation bandwidth of the visual system is approximately 60° (half-bandwidth × 2) and at 11 cycles/degree it has narrowed to approximately 30°. This pattern of results is consistent with estimates from Campbell and

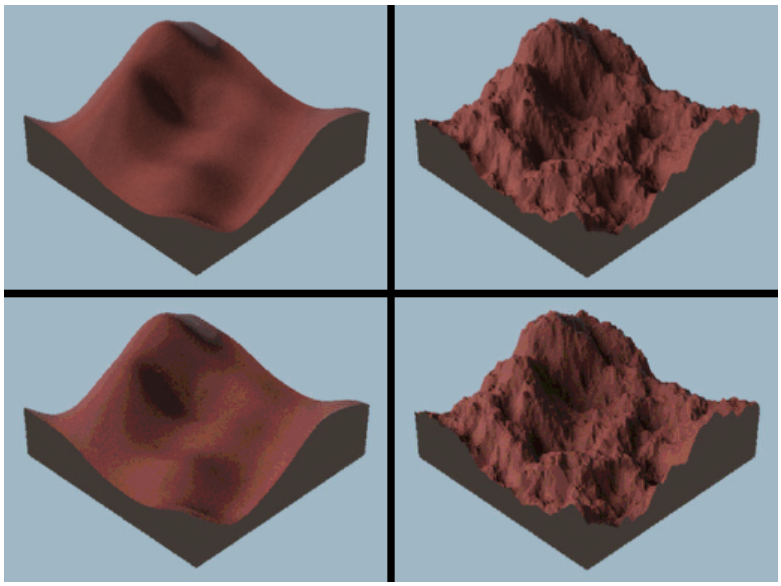

Figure 28: Masking in computer graphics: The upper pair of images are quantized to 8 bits. The lower pair are quantized to 4 bits. Banding is visible in the smooth surface on the lower left but not in the rough surface on the lower right due to masking effects from the visual texture created by the rough surface. From (Bolin95).

Kulikowski's experiments as well as from physiological studies of primate visual cortex (DeValois82).

4.3 Masking

For many years graphics practitioners have observed that visual texture can mask artifacts in images due to noise, aliasing, geometric tesselation, or quantization. A recent example from Bolin (1995) is shown in Figure 28 where banding due to quantization is much more apparent in the smooth surface on the left than in the rough surface on the right. Here the visual texture produced by the rough surface masks the banding artifact.

Masking is a robust perceptual phenomenon that has been studied for more than 30 years by physiologists and psychologists. Masking was first observed in auditory perception (Fletcher52) but analogues in the visual domain were soon discovered (Campbell66, Pantle69). Visual masking can be defined as the situation in which a visual pattern of one type changes the detectability of a pattern of another type. Figure 29 from a classic study by Harmon and Julesz (1973) illustrates the characteristics of visual masking.

A continuous tone photograph of Abraham Lincoln was low-pass filtered to 10 cycles/picture height and then coarsely sampled and quantized to produce the image shown in Figure 29a. Notice how this processing seriously disturbs our ability to recognize the subject. If this blocky image is once again low pass filtered as in Figure 29b, recognition is restored. Thus it first appears that the image discontinuities introduced by high spatial frequencies in the block edges interfere with recognition. However Harmon and Julesz showed that it is not simply high frequencies that disturb recognition, but frequencies adjacent to the picture spectrum. They termed this *critical band masking*. Thus in Figure 29c where spatial frequencies above 40 cycles have been removed, the block edges are softened but recognition is still difficult. However in Figure 29d where frequencies between 12 and 40 cycles have been removed, the block edges are still apparent, but the subject is identifiable. This shows that masking is caused by interactions within a limited spatial frequency band because removal of a critical band of frequencies directly adjacent to the picture's 10 cycle limit eliminates the masking effect but removal of higher frequencies does not.

The visual mechanisms that underlie spatial vision are selective for bands of spatial frequencies and orientations. Interactions between image components within these bands result in masking effects like the ones illustrated in Figures 28 and 29 where the visual response to one component depends upon the presence of other components. The parameters of these masking effects were investigated by Legge and Foley (1980).

Legge and Foley performed a series of experiments to determine how the presence of one grating affects

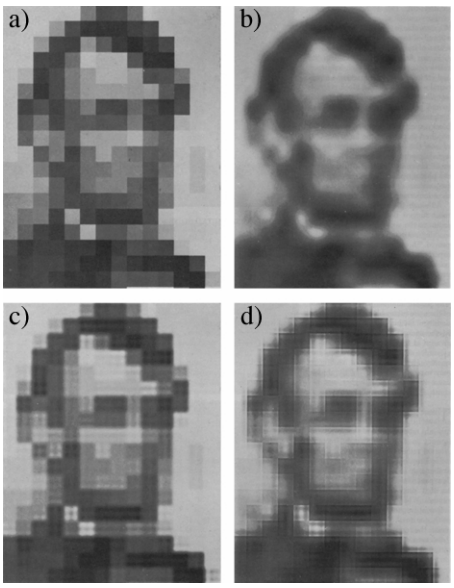

Figure 29: Demonstration of critical band masking: (a) consists of a continuous tone photograph that has been low-pass filtered to 10 cycles/picture-height and then coarsely sampled and quantized to 16 gray levels. This introduces noise into the image spectrum and recognition of the subject is greatly disturbed. In (b) frequencies above 12 cycles have been filtered out removing the blocky appearance and recognition is restored. However, selective removal of parts of the spatial frequency spectrum reveals which noise frequencies mask the image. In (c) frequencies above 40 cycles have been removed. Even though the block edges have been eliminated recognition is still difficult. If however, the band of frequencies adjacent to the picture spectrum from 10 to 40 cycles is removed, the subject can again be recognized. The phenomenon responsible for this is masking within spatial frequency and orientation tuned mechanisms in the visual system. From (Harmon73).

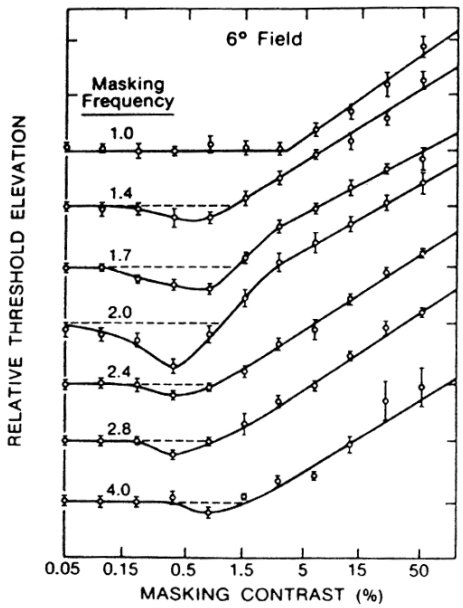

Figure 30: Facilitation and threshold elevation due to masking: Curves show contrast thresholds for a 2.0 cycle/degree sine-wave grating as a function of the masking grating contrast. The individual curves show the results for different spatial frequency masks. Each curve is plotted on its own arbitrary scale. The dotted line through each curve indicates the unmasked threshold for the 2.0 cycle/degree test grating. Note that the curves show a pattern of facilitation or increased sensitivity at low mask contrasts and threshold elevation at higher mask contrasts. From (Legge80).

the detectability of another. The first grating is called the *mask* and the other is the *test*. Their test grating was a sine-wave grating of 2.0 cycles/degree. The masks were phase-coherent sine-wave gratings that ranged in frequency from 1.0 to 4.0 cycles/degree. They measured the threshold contrast necessary to detect the test grating while varying the contrast and spatial frequency of the mask. Their results are shown in Figure 30.

The individual curves show the results for each mask frequency. Each curve is plotted on its own vertical scale showing in arbitrary units, the relative threshold elevation produced by the mask at different mask contrasts. The general form of the results is that very low mask contrasts have no significant effect on the detectability of the test grating, but as the mask contrast is increased, at first the threshold drops showing increased sensitivity or *facilitation* and then rises again showing a loss in sensitivity or *threshold elevation* for high contrast masks. The shape of the threshold elevation curve is evidence of a contrast nonlinearity in the visual system caused by masking. This contrast nonlinearity is an accelerating function at low mask contrasts and a compressive function at higher mask contrasts.

The curves in Figure 30 also shows the spatial frequency tuning of visual masking. Threshold elevation is greatest when the mask and test gratings have the same spatial frequency. As the spatial frequencies of the mask and test become different greater and greater mask contrasts are necessary to produce the same threshold elevation. Since the slopes of the high contrast portions of the curves are close to parallel, the effect on masking of changing the spatial frequency of the mask can be thought of as a horizontal shift in the position of a general masking function. This analysis is described in (Daly92). It has its historical roots in Stiles' *line-element* model of color vision (Stiles78), and a model of spatial vision developed by Graham (1989).

Bibliography

Adelson E.H. (1982). Saturation and adaptation in the rod system. Vision Research, 22, 1299-1312.

Atkinson, R.C. (Ed.) (1988). *Steven's handbook of experimental psychology*. New York: Wiley.

Baker, H.D. (1949). The course of foveal adaptation measured by the threshold intensity increment. Journal of the Optical Society of America, 39, 172-179.

Barlow, H.B. (1979). Reconstructing the Visual Image in Space and Time. Nature, 279, 189-190.

Blakemore, C. and Campbell, F.W. (1969). On the existence of neurones in the human visual system selectively sensitive to the orientation and size of retinal images. J. Physiol., 203, 237-260.

Bolin, M.R. and Meyer, G.M. (1995). A frequency based ray tracer. Proceedings ACM SIGGRAPH '95, 409-418.

Bowmaker, J.K. and Dartnall, H.J.A. (1980). Visual pigments of rods and cones in a human retina. J. Physiol., 298, 501-511.

Braddick, O.J., Campbell, F.W. and Atkinson, J. (1978). Channels in vision: basic aspects, in R. Held, H. Leibowitz, and H.L. Teuber (Eds.), *Handbook of sensory physiology (Vol 8): Perception*, Springer-Verlag.

Campbell, F.W. and Kulikowski J.J. (1966). Orientation selectivity of the human visual system. J. Physiol., 187, 437-445.

Campbell, F.W. and Robson, J.G. (1968). Application of Fourier analysis to the visibility of gratings. J. Physiol., 197, 551-566.

Crawford, B.H. (1947). Visual adaptation in relation to brief conditioning stimuli. Proceedings of the Royal Society of London, Series B, 128, 283-302.

Crick, F.C., Marr, D.C., and Poggio, T. (1980). An Information Processing Approach to Understanding the Visual Cortex. MIT A.I. Memo 557.

Daly, S. (1992). The visual difference predictor: an algorithm for the assessment of image fidelity. Human Vision, Visual Processing and Digital Display, SPIE Vol. 1666, 2-15.

DeValois, R.L., Yund, E.W., and Hepler, N. (1982). The orientation and direction selectivity of cells in macaque visual cortex. Vision Res., 22, 531-544.

DeValois, R.L. and DeValois, K.L. (1975). Neural coding of color. in The Handbook of Perception, Volume 5, Seeing, (Carterette, E.C., and Friedman, M.P. eds.) Academic Press, New York.

Dowling, J.E. and Boycott, B.B. (1966). Organization of the primate retina: electron microscopy. Proc. Royal Soc. Lond. Ser. B., 166, 80-111.

Enroth-Cugell, C. and Robson, J.G. (1966). The contrast sensitivity of retinal ganglion cells of the cat. J. Physiol., 187, 517-552.

Fletcher, H. (1952). *Speech and hearing* (revised ed.). New York: van Nostrand.

Graham, N.V. (1989). *Visual Pattern Analyzers.* New York: Oxford University Press.

Granit R., Munsterhjelm, A., and Zewi, M. (1939). The relation between concentration of visual purple and retinal sensitivity to light during dark adaptation. Journal of Physiology, 96, 31-44.

Gordon, I.E. (1989). *Theories of visual perception.* New York: Wiley.

Harmon, L.D. and Julesz, B. (1973). Masking in visual recognition: effects of two-dimensional filtered noise. Science, 180, 1194-1197.

Hecht, S. (1934). Vision II: the nature of the photoreceptor process. In C. Murchison (Ed.), A handbook of general experimental psychology. Worchester, Massachusetts: Clark University Press.

Hecht, S., Shlaer, S., & Pirenne, M. (1942). Energy, quanta, and vision. Journal of General Physiology, 25, 891-840.

Hubel, D.H. and Wiesel, T.N. (1962). Receptive fields, binocular interaction, and functional architecture in the cat's visual cortex. J. Physiol., 160, 106-154.

Hubel, D.H. and Wiesel, T.N. (1968). Receptive fields and functional architecture of monkey striate cortex. J. Physiol., 195, 215-243.

Hurvich, L. (1981). *Color Vision.* Sunderland, MA: Sinauer Assoc.

Kennedy, D. (1963) Inhibition in visual systems. Sci. Am., July 1963.

Kuffler, S.W. (1953). Discharge patterns and functional organization of the mammalian retina. J. Neurophysiol., 16, 37-68.

Legge, G.E. and Foley, J.M. (1980). Contrast masking in human vision. J. Opt. Soc. Am., 70, 1458-1470.

Lennie, P. (1984). Recent developments in the neurophysiology of color. Trends in Neuroscience, 7, 243-248.

Livingstone, M.S., and Hubel, D.H. (1984). Anatomy and physiology of a color system in the primate visual cortex. J. Neuroscience, 4, 309-356.

Livingstone, M.S., and Hubel, D.H. (1988). Segregation of form, color, movement and depth, anatomy, physiology and perception. Science, 240, 740-750.

Marr, D., Poggio, T., and Hildreth E. (1980). Smallest Channel in Early Human Vision. J. Opt. Soc. Am., 70(7), 868-870.

Michael, C.R. (1969) Retinal processing of visual images. Sci. Am., May 1969.

Mishkin, M., Ungerleider, L.G., and Macko, K.A. (1983). Object vision and spatial vision: two critical pathways. Trends in Neuroscience, 6, 414-417.

Osterberg, G. (1935). Topography of the Layer of Rods and Cones in the Human Retina. Acta. Ophthal. Suppl., 6 11-97.

Pantle, A. and Sekuler, R.W. (1969). Contrast response of human visual mechanisms sensitive to orientation and direction of motion. Vision Res., 9, 397-406.

Phillips, G.C. and Wilson H.R. (1984). Orientation bandwidths of spatial mechanisms measured by masking. J. Opt. Soc. Am. A, 1, 226-232.

Pirenne, M.H. (1967). *Vision and the eye.* London: Chapman and Hall.

Pugh, E.N. (1988). Vision: physics and retinal physiology, In R.C. Atkinson (Ed.), Steven's handbook of experimental psychology, (2nd edition). New York: Wiley.

Ratliff, F. (1965). *Mach Bands: Quantitative Studies on Neural Networks in the Retina.* San Francisco: Holden-Day.

Riggs, L.A. (1971) Vision. In J.W. Kling & L.A. Riggs (Eds.), Woodworth and Schlosberg's Experimental Psychology , (3rd edition). New York: Holt, Rinehart, and Winston.

Schiffman, H.R. (1982). *Sensation and Perception* (2nd ed.). New York: Wiley.

Sekuler, R., and Blake, R. (1994). *Perception.* New York: McGraw-Hill.

Shaler, S. (1937). The relation between visual acuity and illumination. Journal of General Physiology, 21, 165-188.

Spillman, L., & Werner, J.S. (Eds.) (1990). Visual perception: the neurophysiological foundations. SanDiego: Academic Press.

Stiles, W.S. (1978). *Mechanisms of Color Vision.* London: Academic Press.

Snyder, A.W., and Williams, W.H. (1977). Photoreceptor Diameter and Spacing for Highest Resolving Power. J. Opt. Soc. Am., 67(5), 696-698.

Thomas, J.P. (1975). Spatial Resolution and Spatial Interaction. pp. 233-263 in The Handbook of Perception, Volume 5, Seeing, (Carterette, E.C., and Friedman, M.P. eds.) Academic Press, New York, 1975.

Walls, G.L. (1942). The vertebrate eye and its adaptive radiation. Cranbrook Institute of Science, Bull. 19, Bloomfield Hills, Michigan.

Watt, R.J., and Morgan, M.J. (1983). Mechanisms Responsible for the Assessment of Visual Location: Theory and Evidence. Vis. Res., 23, 97-109.

Westheimer, G. (1977). Spatial Frequency and Light Spread Descriptions of Visual Acuity and Hyperacuity. J. Opt. Soc. Am., 1977, 67(2), 207-212.

Wilson, H.R. and Gelb, D.J. (1984). Modified line-element theory for spatial-frequency and width discrimination. J. Opt. Soc. Am. A, 1, 124-131.

Wilson, H.R. (1991). Psychophysical models of spatial vision and hyperacuity. in D. Regan (Ed.) *Spatial Vision*, Vol. 10, Vision and Visual Dysfunction. Boca Raton, FL, CRC Press.

Wyszecki G. & Stiles W.S. (1982). *Color Science: Concepts and Methods, Quantitative Data and Formulae* (2nd edition). New York: Wiley.

Zrenner, E. and Gouras, P. (1983). Cone opponency in tonic ganglion cells and its variation with eccentricity in rhesus monkey retina. In J. Mollon and T. Sharpe (Eds.) *Color Vision: Physiology and Psychophysics.* New York: Academic Press.